

Boundary-Condition Quantum Mechanics III: A Stochastic Growth Model for Causal Event Chains and the Emergence of Inertia

Peter M. Ferguson
Independent Researcher

November 19, 2025

Abstract

This work presents the technical development of the **BCQM III** framework, which posits spacetime as an emergent causal graph of irreversible “Events”. We define the mathematical formalism for the q-wave, the informational field that governs the graph’s growth, and detail a stochastic algorithm that simulates the creation of a particle’s worldline. The primary result of this paper is to demonstrate, through both simulation and analytical argument, that the classical principle of inertia is an inevitable statistical consequence of the q-wave’s phase coherence. This provides the foundational engine for the quantitative predictions of the BCQM framework. *Clarification.* In this paper, “advanced” refers only to the advanced Green’s-function branch used in BCQM to keep the amplitude description time-symmetric. It is *not* evolution “back in time,” entails no future-to-past influence, and cannot be used for signalling; all operational ordering is along the ordinary chronological axis. Outcome weights arise from pairing the forward (t^+) and coherence/advanced (t^-) contributions at the candidate event, $w = |K|^2$; in the normalised sampling step the advanced factor is absorbed into the denominator.

1 The Q-Wave as a Propensity Field

Interpretation note (no retrocausality). Dynamics and realisation here use the retarded component ψ^+ . Any mention of an “advanced” branch is purely mathematical—amplitude bookkeeping to respect time symmetry—and is not read as a physical process propagating backwards in time. Causes, records, and interventions remain ordered along laboratory time.

1.1 Retarded component and invariant action phase

We assign the retarded propensity to each candidate successor event $E' \in \partial\mathcal{F}_n$ via the invariant action increment:

$$\psi^+(E') = \mathcal{N}^{-1/2} \exp\left(\frac{i}{\hbar} \Delta S(E', E_n)\right), \quad \Delta S := p_\mu \Delta x^\mu, \quad (1)$$

with $\Delta x^\mu := x'^\mu - x_n^\mu$. For a free massive particle, $\Delta S = -mc^2 \Delta\tau$; for massless propagation take $p_\mu = \hbar k_\mu$ and $\Delta S = \hbar k_\mu \Delta x^\mu$. The normalisation factor \mathcal{N} ensures either $\sum_{E' \in \partial\mathcal{F}_n} |\psi^+(E')|^2 = 1$ (discrete frontier) or $\int_{\partial\mathcal{F}_n} |\psi^+|^2 \mu_n(dE') = 1$ (continuous frontier), where μ_n is the invariant measure induced on the frontier.

Realisation law (preview). Given the frontier $\partial\mathcal{F}_n$, the next realised Event is drawn according to

$$\mathbb{P}(E_{n+1} = E') = \frac{|\psi^+(E')|^2}{\sum_{E'' \in \partial\mathcal{F}_n} |\psi^+(E'')|^2}, \quad (2)$$

a weighted random choice. This implements intrinsic stochasticity; it is not a drift to the dominant channel.

t^+/t^- pairing (probability law). The weighting in (2) is the pairing of the forward (t^+) and coherence/advanced (t^-) contributions at the candidate event E' , i.e.

$$w(E') = \psi^+(E') \psi^-(E') = |\psi^+(E')|^2, \quad \psi^-(E') := \psi^+(E')^*.$$

In the normalised sampling step any common multiplicative factor in ψ^- cancels between numerator and denominator; this is what is meant by saying the advanced factor is “set to 1” (absorbed into the normalisation). We *apply* the modulus–square law here (motivated by $t^+ - t^-$ pairing); the *derivation* under explicit axioms is provided in *Analytical Proofs for BCQM* [1].

See also App. ?? for the t^+/t^- pairing and the “set to 1” normalisation shorthand.

Remark. The advanced component is retained only as the conjugate co-contribution at the candidate event: $\psi^-(E') := \psi^+(E')^*$. The outcome weight is therefore the t^+/t^- pairing $w(E') = \psi^+(E') \psi^-(E') = |\psi^+(E')|^2$, and the normalised sampling law follows directly. When authors say the advanced factor is “set to 1”, this is shorthand for its absorption into the normalisation at the probability step. We *apply* the modulus–square law here (motivated by $t^+ - t^-$ pairing); the *derivation* under explicit axioms is provided in *Analytical Proofs for BCQM* [1].

Clarification. The advanced branch is retained to enforce time-symmetric pairing at the event ($\psi^- = \psi^{+*}$); propagation and local dynamics use ψ^+ on the frontier. There is no retrocausal signalling: realised outcomes do not depend on future settings.

The BCQM II framework [2] proposes that reality is a growing causal graph of irreversible quantum events. The growth of this graph is not arbitrary; it is governed by an information field, the q-wave, which serves as a blueprint for potentiality. To construct a predictive model, we must first translate this conceptual role into a concrete mathematical object.

1.2 State Representation and the Future Boundary

In our event-based ontology, the state of a particle is defined entirely by its most recent realised **Event**.

- The state of a particle is specified by its last Event, E_n , which is characterized by its emergent spacetime coordinates, $x_n^\mu = (ct_n, \vec{x}_n)$, and its four-momentum, $p^\mu = (E/c, \vec{p})$.
- The **Future Boundary** is the set of all possible Events, $\{E_{n+1}\}$, that are causally accessible from E_n in a single “tick”. For the purpose of this model, we can visualize this as a discrete set of adjacent nodes on an underlying computational lattice.

The q-wave amplitude on the future boundary is the retarded function $\psi^+(E_{n+1})$, and event growth uses ψ^+ alone.

Remark. The advanced component ψ^- is retained to reflect BCQM’s two-boundary perspective; it constrains propensities but does not generate new events. Event growth uses ψ^+ . For a single, free particle, the advanced component, ψ^- , which enforces global consistency, is uniform and can be absorbed into the normalisation constant. The crucial dynamics are contained in the retarded component, ψ^+ .

No retrocausality. Probabilities on the frontier are computed from amplitudes available at the current step. Changing future settings cannot affect already realised Events; reduced statistics at one site remain independent of any future choice elsewhere.

1.3 The Mathematical Form of the Retarded Q-Wave (ψ^+)

The retarded component, ψ^+ , propagates from the definite past Event, E_n , to the field of potential future Events, $\{E_{n+1}\}$. For a free particle, this propagation must take the form of a discrete plane wave.

The general form is:

$$\psi^+(E_{n+1}) = A \cdot \exp(i\phi) \quad (3)$$

where A is a normalisation amplitude and ϕ is the phase. To ensure the laws of our emergent spacetime are consistent with special relativity, the phase ϕ must be a Lorentz-invariant scalar. We define the phase using the dot product of the four-momentum, p^μ , and the four-displacement, $\Delta x^\mu = x_{n+1}^\mu - x_n^\mu$:

$$\phi = -\frac{p_\mu \Delta x^\mu}{\hbar} \quad (4)$$

Using the $(+,-,-,-)$ metric signature, the complete mathematical formula for the retarded component of the q-wave is:

$$\psi^+(E_{n+1}) = A \cdot \exp \left[\frac{i}{\hbar} (\vec{p} \cdot (\vec{x}_{n+1} - \vec{x}_n) - E(t_{n+1} - t_n)) \right] \quad (5)$$

This choice is mandated by relativistic invariance and its direct connection to the quantum mechanical propagator. It is this phase structure that gives rise to the interference phenomena that will be shown to produce inertia.

Regulator. Any underlying computational lattice is used solely as a regulator; our intent is the continuum (or Lorentz-covariant Poisson-sprinkled) limit, so physical predictions do not depend on a particular slicing or grid.

2 A Stochastic Graph-Growth Algorithm

With a concrete mathematical form for the q-wave, we now define the "engine" of the theory: a computational algorithm that simulates the growth of a particle's causal event chain. A Monte Carlo method is the natural approach for modeling this process. *Causality note.* The graph-growth procedure is strictly forward-ordered: each *realisation* conditions only on established records and the current frontier. No future-to-past influence is assumed or permitted.

Companion note. A full development of the minimal primitives and the hop-bounded *realisation law* is given in the companion "Primitives" note [3].

2.1 The Algorithm

We present the process in the form of pseudocode (Algorithm 1).

Propagation-and-realisation window. We parameterise evolution by the particle's proper time $\Delta\tau$ (for massive trajectories) or by an affine parameter (for massless ones). Between collapses, the propensity field is represented as a narrow wavepacket centred at the realised event E_n with phase gradient set by p^μ . The packet is propagated coherently for a finite window $\Delta\tau$, which in the simulation corresponds to a thin spatial slab of thickness $L = v_0 \Delta\tau$ in the lab frame, where v_0 is the characteristic speed used to set the lattice spacing and time step. Event realisation is then sampled once from $|\psi^+|^2$ on this frontier slab.

$$\psi_n(x) = \mathcal{N} \exp \left[-\frac{(x-x_n)^2}{4\sigma^2} + \frac{i}{\hbar} p_\mu (x^\mu - x_n^\mu) \right]. \quad (6)$$

The packet is propagated coherently for a finite window $\Delta\tau$ (or L micro-steps of a short-time kernel K), and the next Event is then sampled once from $|\psi_+|^2$ on the frontier. This delayed realisation permits multi-path interference within the window and yields a geodesic bias consistent with the stationary-phase argument.

Algorithm 1 Stochastic Event Chain Growth

```

1: function GROWEVENTCHAIN( $E_0, p^\mu, N_{ticks}, \sigma, \Delta\tau, L$ )
2:    $Chain \leftarrow [E_0]$                                  $\triangleright$  Initialize the chain with the first Event
3:    $E_{current} \leftarrow E_0$ 
4:   for  $n \leftarrow 1$  to  $N_{ticks}$  do
5:      $Packet \leftarrow \text{InitPacket}(E_{current}, p^\mu, \sigma)$            $\triangleright$  Narrow Gaussian, Eq. (6)
6:      $Packet \leftarrow \text{Propagate}(Packet, \Delta\tau, L, K)$   $\triangleright$  Coherent window of duration  $\Delta\tau$  and slab
   thickness  $L = v_0\Delta\tau$  via short-time kernel  $K$ 
7:      $Boundary \leftarrow \text{GetFutureBoundary}(Packet)$   $\triangleright$  Candidates on the thin slab (frontier)
8:      $Probabilities \leftarrow \text{FrontierProbabilities}(Packet, Boundary)$   $\triangleright$  applied law:  $P \propto |\psi_+|^2$ 
   (derivation in [1])
9:      $E_{selected} \leftarrow \text{StochasticSelect}(Boundary, Probabilities)$   $\triangleright$  single realisation / collapse
10:     $Chain.append(E_{selected})$ 
11:     $E_{current} \leftarrow E_{selected}$ 
12:   end for
13:   return  $Chain$ 
14: end function

```

2.2 Interpretation of the Steps

2.3 Regulator and continuum limit tied to W_{coh}

We make explicit how the lattice and windowing co-move so that the model admits a clean continuum limit and a clear dependence on the coherence horizon W_{coh} . Let a be the lattice spacing and Δt the time per growth step, and define $v_0 = a/\Delta t$. Choose per-step attenuation and a real window

$$\rho = \exp\left(-\frac{\Delta t}{2W_{coh}}\right), \quad g(k; \ell_{env}) = \exp\left(-\frac{k a}{\ell_{env}}\right), \quad \ell_{env} = \beta v_0 W_{coh}, \quad \beta > 0. \quad (7)$$

Notation. We reserve $w(x)$ for local outcome weights (the $t^+ - t^-$ pairing), W_{coh} for the coherence horizon, and ℓ_{env} for the environment window length in the regulator.

Take the continuum limit

$$a, \Delta t \rightarrow 0, \quad v_0 = \frac{a}{\Delta t} \text{ fixed}, \quad \ell_{env} = \beta v_0 W_{coh} \text{ fixed}, \quad (8)$$

so that $k a$ is a path arclength and g remains a positive, real window tied to W_{coh} . Under this scaling, the linear-response analysis yields the emergent inertial parameter $m_{\text{eff}} \propto W_{coh}^{-2}$ up to geometry and phase-averaging factors. We introduce a real, positive **environment window length** ℓ_{env} , which sets the exponential damping of long paths in the regulator. With $\ell_{env} = \beta v_0 W_{coh}$, the window scale co-moves with the coherence horizon.

- **Propagation (Lines 5-6):** This loop implements the retarded component of the q-wave. It "paints" the future boundary with complex amplitudes, creating a field of potentiality.
- **Realisation (Lines 7-9):** This is the physical collapse at the coherence horizon W_{coh} . We apply the modulus-square (Born) law, $P \propto |\psi_+|^2$; the derivation under explicit axioms is provided in *Analytical Proofs for BCQM* [1]. A single, definite outcome is then realised, making history definite.

- **Update** (Line 10): The realised Event is added to the history of the particle, and the process repeats from this new state.

This algorithm provides the core mechanism of the BCQM III framework. In the following section, we analyze the statistical properties of the chains it produces to demonstrate the emergence of classical kinematics.

3 Inertia as a Consequence of Phase Coherence

Equivalently, we use the invariant action phase $\exp(i \Delta S/\hbar)$ with $\Delta S = p_\mu \Delta x^\mu$ as established in Section 1.

This section presents the central result of this paper: the demonstration that the classical principle of inertia is an inevitable statistical consequence of the quantum dynamics defined by the q-wave and the growth algorithm. Inertia is not a fundamental law, but an emergent property of phase coherence. *Two-time symmetry vs. causal order.* Time-symmetric amplitude bookkeeping (when used) does not imply retrocausal dynamics; the emergent geodesic arises from many forward-ordered *realisations* along t^+ .

3.1 The Physical Principle: Constructive and Destructive Interference

The stochastic *realisation* process detailed in Algorithm 1 does not produce a simple random walk. The choice of the next Event is biased by the phase of the q-wave. For a free particle, the q-wave (Eq. 5) takes the form of a plane wave. The probability of realising a successor Event is highest where the amplitudes for all contributing paths interfere constructively.

- **The Path of Maximum Coherence:** The path where the phase remains stationary is the one that lies along the direction of the particle's momentum, \vec{p} . Along this "straight line" geodesic, the phase accumulates linearly, and all adjacent potential paths have nearly the same phase, leading to maximum constructive interference.
- **Suppression of Deviations:** Any potential path that deviates significantly from this geodesic will involve a rapid change in phase. The amplitudes for these paths will destructively interfere with each other, leading to a suppressed probability of being *realised*.

Therefore, while any single "tick" is probabilistic and exhibits a quantum jitter, the overwhelming statistical trend is for the event-chain to follow the path of maximum phase coherence.

3.2 Simulation Results and the Emergence of Geodesics

All simulations were performed using the parameters detailed in Appendix ??.

As a visual summary, Figure 1 shows many realised threads (thin), their mean (thick), and a 95% band at $b = 0$; the linear growth of the mean for $t \ll W_{\text{coh}}$ foreshadows the conserved coarse velocity established below.

Empirical checks. Figure 2 reports the ensemble mean displacement at $b = 0$. The linear growth for $t \ll W_{\text{coh}}$ confirms conserved coarse velocity in the unbiased regime, in agreement with the inertial coarse-graining of §3. Figure 3 shows the small-drive response sweep, where an effective inertial parameter m_{eff} is extracted from the slope $d\langle v \rangle / db$; a power-law dependence on W_{coh} is evident on log-log axes and is consistent with the prediction $m_{\text{eff}} \propto W_{\text{coh}}^{-2}$ (derived in Appendix ??) and shown to be a robust result insensitive to numerical choices (see Appendix ?? for stability analysis), under the regulator scaling stated earlier. Finally, Figure 4 plots the velocity autocorrelation against the scaled lag $\text{lag}/W_{\text{coh}}$ and exhibits a collapse of the curves,

indicating a correlation timescale proportional to W_{coh} and thereby supporting the window-tied dynamics.

Operator-theoretic derivations and proof details are provided in *Analytical Proofs for BCQM* [1].

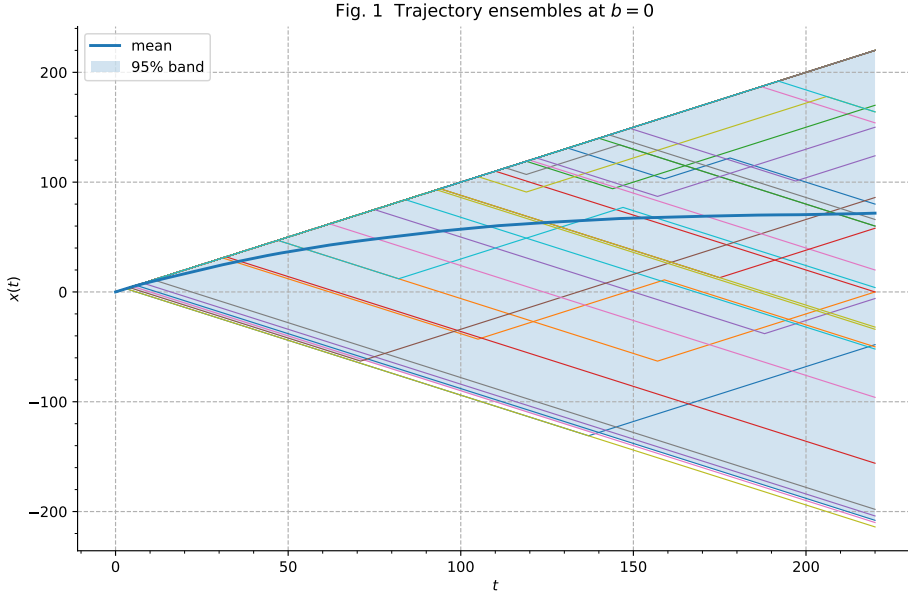


Figure 1: Trajectory ensembles at $b = 0$: multiple realised threads (thin lines) with mean (thick line) and a 95% band (shaded). The linear growth of the mean for $t \ll W_{\text{coh}}$ foreshadows the conserved coarse velocity established below.

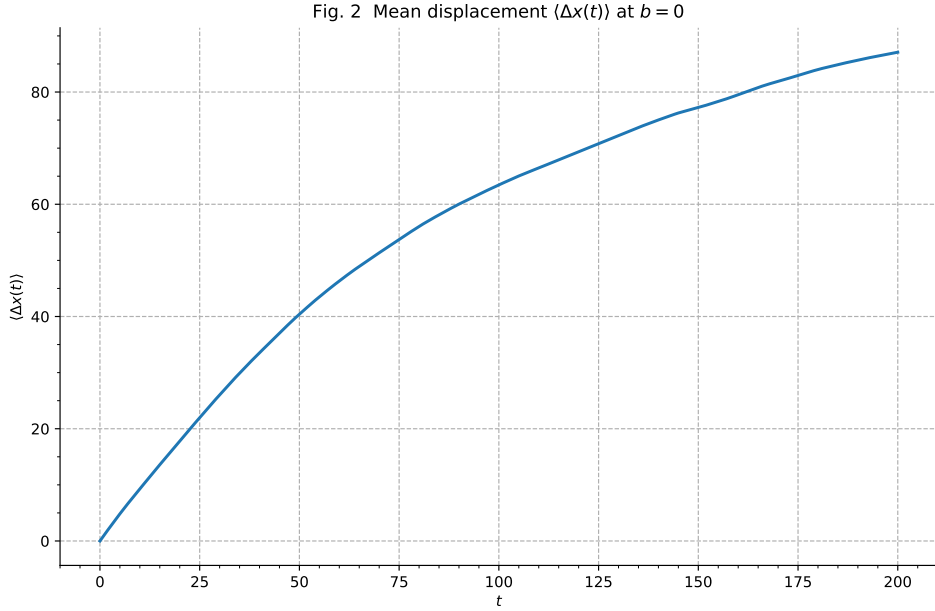


Figure 2: Mean displacement $\mathbb{E}[\Delta x(t)]$ at $b = 0$, showing conserved coarse velocity over the window $t \ll W_{\text{coh}}$.

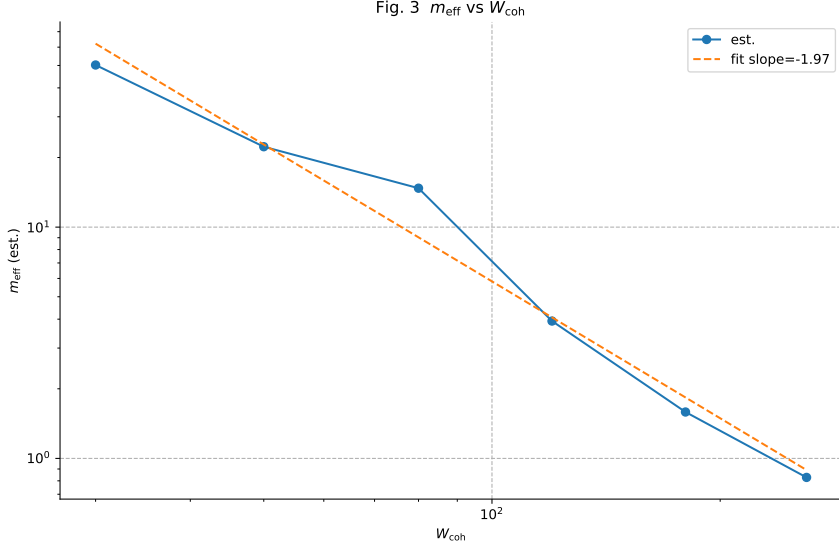


Figure 3: Effective mass versus coherence horizon. We plot $m_{\text{eff}}(W_{\text{coh}})$ extracted from the linear response to small drive b as a function of W_{coh} on log–log axes. The best-fit straight line (solid) has a slope close to -2 , consistent with the theoretical scaling $m_{\text{eff}} \propto W_{\text{coh}}^{-2}$.

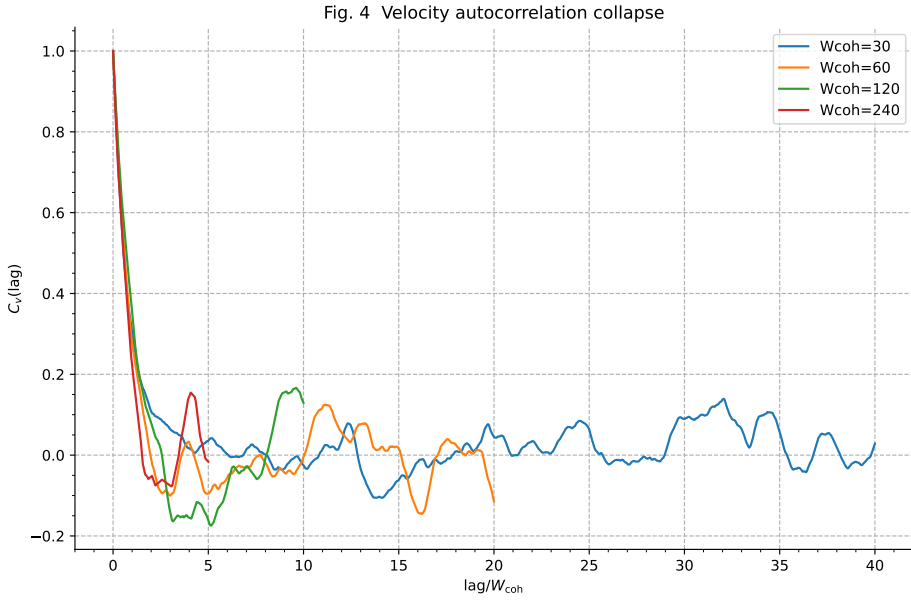


Figure 4: Velocity autocorrelation $C_v(\text{lag})$ plotted against the scaled lag $\text{lag}/W_{\text{coh}}$ for multiple W_{coh} . The curves collapse, indicating a correlation timescale proportional to W_{coh} .

Companion note. This demonstrates that the classical, deterministic trajectory of a particle is the statistical mean of an underlying quantum-stochastic process. The geodesic is an emergent property.

3.3 Connection to the Path Integral Formalism

This result can be understood analytically by drawing a parallel to the Feynman path integral formalism. The probability of a particle transitioning between two points is the squared modulus

of the sum of amplitudes for all possible paths between them.

Interference across a coherent window. In practice, interference arises because the propensity packet is propagated *coherently* for a finite window $\Delta\tau$ (or L short sub-steps of a kernel K) before a single *realisation* is made. Equivalently, amplitudes to each candidate on the thin slab are summed via repeated application of K , so that stationary-phase contributions dominate and bias the realised event toward the geodesic direction.

$$P(b, a) = \left| \sum_{\text{paths}} e^{iS[\text{path}]/\hbar} \right|^2 \quad (9)$$

In the classical limit, the path that dominates this sum is the one for which the action, S , is stationary—the principle of least action. Our model is the discrete, event-by-event realization of this principle. The "path of maximum phase coherence" is precisely the path of stationary action, and our stochastic algorithm is the mechanism that ensures this path is the most probable outcome.

The simulation exposes explicit control knobs—packet width σ , propagation window $\Delta\tau$ (or step count L), and a reproducibility seed—whose combined effect sets the jitter amplitude around the mean path; this amplitude is analysed in Paper IV as the inertial-noise PSD governed by the horizon W_{coh} .

Reproducibility and code availability. A reference implementation and configuration files (matching Algorithm 1 step-for-step) are available in a public repository with a `README.md`, exact commands to regenerate Figs. 1–4, and a `CITATION.cff` [4]. Sweep configs and outputs are archived with a DOI.

Scope, limitations, and hand-off to BCQM IV

This paper works entirely within the *emergent spacetime* regime of the BCQM programme. We assume that, at sufficiently large scales, the web of quantum events admits an effective Minkowski description with a well-defined proper time and action functional. In particular, the phase structure used in Algorithm 1—the increment $\Delta S \approx p_\mu \Delta x^\mu$ and its free-particle specialisation $\Delta S \approx -mc^2 \Delta\tau$ —is taken as given at this continuum level. Our goal here is not to derive this effective action from the primitive event-graph rules, but to show that, *given* such an emergent background, a finite coherence horizon and a hop-bounded growth law already suffice to produce classical inertial motion and an effective mass scaling $m_{\text{eff}} \propto W_{\text{coh}}^{-2}$. The derivation of the continuum phase structure itself—and of the underlying Lorentzian geometry and dimensionality—from the minimal BCQM primitives is deferred to future work in this series (BCQM IV and V).

A natural objection is that using a phase structure $\Delta S \approx p_\mu \Delta x^\mu$ before deriving spacetime might be circular. It is not. This is standard effective field theory methodology: one works at a given scale with the appropriate degrees of freedom and coupling structure, and tackles the UV completion or emergent infrared description separately. Just as lattice QCD uses discrete Wilson actions chosen to flow to the continuum QCD Lagrangian through universality, we conjecture that generic local graph-phase rules—subject to appropriate symmetry and locality constraints—will reproduce the relativistic action in the emergent regime. The micro-to-macro universality argument, including the emergence of 3 + 1 dimensions and Lorentz invariance as coarse-grained statistical symmetries, is the subject of BCQM IV–V. Here we provide the engine that operates on emergent spacetime; the derivation of that spacetime from primitives is a separate (and harder) problem.

The jitter power spectral density and the inertial noise floor, while motivated here by the event-chain growth picture, are quantified in the follow-on work (BCQM IV). The present paper establishes the stochastic growth model and the scaling $m_{\text{eff}} \propto W_{\text{coh}}^{-2}$; spectral character and experimental readout are deferred.

References

- [1] Peter M. Ferguson. *Analytical Proofs for BCQM*. 2025. DOI: [10.5281/zenodo.17242311](https://doi.org/10.5281/zenodo.17242311). URL: <https://doi.org/10.5281/zenodo.17242311>.
- [2] Peter M. Ferguson. *Boundary-Condition Quantum Mechanics II: From Quantum Events to Spacetime*. 2025. DOI: [10.5281/zenodo.17398294](https://doi.org/10.5281/zenodo.17398294). URL: <https://doi.org/10.5281/zenodo.17398294>.
- [3] Peter M. Ferguson. *Minimal amplitude-first primitives for BCQM: events, directed edges, and complex amplitudes with a single hop-bounded selection rule*. 2025. DOI: [10.5281/zenodo.17495038](https://doi.org/10.5281/zenodo.17495038). URL: <https://doi.org/10.5281/zenodo.17495038>.
- [4] Peter M. Ferguson. *BCQM III Simulation & Figures Code*. Version 1.0.1. 2025. DOI: [10.5281/zenodo.17632820](https://doi.org/10.5281/zenodo.17632820). URL: <https://doi.org/10.5281/zenodo.17632820>.
- [5] Zlatko K. Minev et al. “To catch and reverse a quantum jump mid-flight”. In: *Nature* 570.7760 (2019), pp. 200–204. DOI: [10.1038/s41586-019-1287-z](https://doi.org/10.1038/s41586-019-1287-z).
- [6] Göran Lindblad. “On the Generators of Quantum Dynamical Semigroups”. In: *Communications in Mathematical Physics* 48.2 (1976), pp. 119–130. DOI: [10.1007/BF01608499](https://doi.org/10.1007/BF01608499). URL: <https://doi.org/10.1007/BF01608499>.
- [7] Vittorio Gorini, Andrzej Kossakowski, and E. C. G. Sudarshan. “Completely positive dynamical semigroups of N-level systems”. In: *Journal of Mathematical Physics* 17.5 (1976), pp. 821–825. DOI: [10.1063/1.522979](https://doi.org/10.1063/1.522979). URL: <https://doi.org/10.1063/1.522979>.